A few points on acoustic waves and spray dynamics

Marc Massot

Professor, Ecole Centrale Paris
Laboratoire EM2C - UPR 288
Grande Voie des Vignes
92295 CHATENAY-MALABRY
massot@em2c.ecp.fr

1 Configuration - equations

We consider an oscillating field of gaseous phase velocity carrying a spray of monodisperse droplets under the assumption of one-way coupling. We introduce a few parameters; the oscillating gaseous field is given by

$$U(t,x) = A\,\sin\left(\frac{2\pi\,(x - c\,t)}{\lambda}\right). \tag{1}$$

The spray is described by a number distribution function $f(t,x,v)$ satisfying the usual Williams spray equation

$$\partial_t f + v.\partial_x f + \partial_v(F(t,x,v)f) = 0. \tag{2}$$

where the drag force is considered under the Stokes regime to be

$$F(t,x,v) = \frac{U(t,x) - v}{\tau_p(t)} \tag{3}$$

where eventually, the droplet Stokes time τ_p can evolve qdue to evaporation.

We consider also the initial distribution f^0 to be monokinetic $f^0 = n^0(x)\,\delta(v - v_d^0(t,x))$, so that, as long as the velocity field v_d^0 remains a regular field, there is an equivalence between the original equation (2) and the semi-kinetic formulation :

$$\left\{\begin{array}{rl} \partial_t n + \partial_x(n\,v_d) & = 0 \\ \partial_t(n\,v_d) + \partial_x\left(\dfrac{(n\,v_d)^2}{n}\right) & = n\dfrac{U - v_d}{\tau_p(t)}, \end{array}\right. \tag{4}$$

for which the smooth velocity field satisfies the Burgers equation, independently of the density one :

$$\partial_t v_d + \partial_x(v_d^2) = \frac{U - v_d}{\tau_p(t)}. \tag{5}$$

The initial droplet velocity field is going to be taken under the form of

$$v_d^0(x) = \mathcal{A}^0\,\sin\left(r\,\frac{2\pi\,x}{\lambda} + \phi\right). \tag{6}$$

where r denotes the frequency ratio, $\mathcal{A}^0$ the initial amplitude of the droplet velocity variations and ϕ the phase shift.

In the case of an evaporating monodisperse spray, we then have a variable droplet relaxation time $\tau_p(t)$ which will be written, in the context of d^2 law as $\tau_p^0(1 - t/\tau_v)$, which means that we introduce another time scale in the problem.

2 The caracteristic curves

In the following we will intensively use the evolution equations along the caracteristic curves which are defined by :

$$\left\{ \begin{array}{ll} \mathrm{d}_t X_p & = V_p, \\ \mathrm{d}_t V_p & = \dfrac{U(t, X_p) - V_p}{\tau_p(t)}, \end{array} \right. \tag{7}$$

where it should be noticed that the non-linear coupling between the two fields is contained in the fact that the gaseous velocity field U is only sampled by the droplet trajectory at X_p. The initial conditions are defined by :

$$\left\{ \begin{array}{ll} X_p(0) & = X_p^0, \\ V_p(0) & = V_p^0 = v_d^0(X_p^0), \end{array} \right. \tag{8}$$

since the initial distribution is monokinetic; thus the caracteristic curves are the integral curves of the vector field defined by (7). They in fact are parametrized by the initial spatial coordinate so that we will adopt the notation $(X_p, V_p)^t(t, X_p^0)$. Under some standard conditions on the regularity of the field U, the caracteristic curves exist and are well-defined for all time and spatial initial condition. However, as soon as some caracteristic curves cross in the only spatial projection, the distribution ceases to be monokinetic and the former equivalence is not valid any more (in fact the caracteristics never cross in the (x, v) phase space so that the distribution admits many velocities at a point where the spatial projection of the caracteristics cross). Some precise examples will be provided in the following.

3 Relaxation variables

We introduce the relaxation variables both at the kinetic level (2) $w = v \exp(-t/\tau_p)$ and at the semi-kinetic level (4) $w_d = v_d \exp(-t/\tau_p)$ in the non-evaporating framework, as well as a new time variable $\tau = \tau_p(1 - \exp(-t/\tau_p))$ so that $\exp(t/\tau_p) = 1/(1 - \tau/\tau_p)$ and $t = -\tau_p \log(1 - \tau/\tau_p)$. One can check that the equation (2) and the system (4) then read :

$$\partial_\tau f^{\mathrm{rel}} + w.\partial_x f^{\mathrm{rel}} + \partial_v \left(\frac{U(\tau, x)}{\tau_p(1 - \tau/\tau_p)^2} f^{\mathrm{rel}} \right) = 0. \tag{9}$$

and

$$\left\{ \begin{array}{rl} \partial_\tau n + \partial_x(n\, w_d) & = 0, \\ \partial_\tau(n\, w_d) + \partial_x \left(\dfrac{(n\, w_d)^2}{n} \right) & = n \dfrac{U}{\tau_p(1 - \tau/\tau_p)^2}, \end{array} \right. \tag{10}$$

which, again, admits the same caracteristic curves in the (x, w, t) tri-dimensional phase space as long as the solution of the semi-kinetic model remains smooth enough.

As far as the evaporating case is concerned, the change of variable is different, because of the evolution of the relaxation time τ_p with time. One takes

$$w_d = \frac{v}{(1 - t/\tau_v)^\alpha}, \quad \alpha = \tau_v/\tau_p \tag{11}$$

and a new time variable

$$\tau = \frac{\tau_v}{1+\alpha}\left[1 - \left(1 - \frac{t}{\tau_v}\right)^{1+\alpha}\right], \tag{12}$$

or differently written :

$$\frac{\tau}{\tau_p}\frac{1+\alpha}{\alpha} = 1 - \left(1 - \frac{t}{\tau_v}\right)^{1+\alpha}.$$

The correspondance between the two times is plotted for various α in Figure 1.

One can check that the equation (2) and the system (4) then read :

$$\partial_\tau f^{\mathrm{rel}} + w.\partial_x f^{\mathrm{rel}} + \partial_v \left(\frac{U(\tau, x)}{\tau_p(1 - \frac{\tau}{\tau_p}\frac{1+\alpha}{\alpha})^{\frac{2\alpha+1}{\alpha+1}}} f^{\mathrm{rel}} \right) = 0. \tag{13}$$

and

$$\begin{cases} \partial_\tau n + \partial_x(n\, w_d) &= 0, \\ \partial_\tau(n\, w_d) + \partial_x\left(\dfrac{(n\, w_d)^2}{n}\right) &= n\dfrac{U}{\tau_p\left(1 - \dfrac{\tau}{\tau_p}\dfrac{1+\alpha}{\alpha}\right)^{\frac{2\alpha+1}{\alpha+1}}}, \end{cases} \tag{14}$$

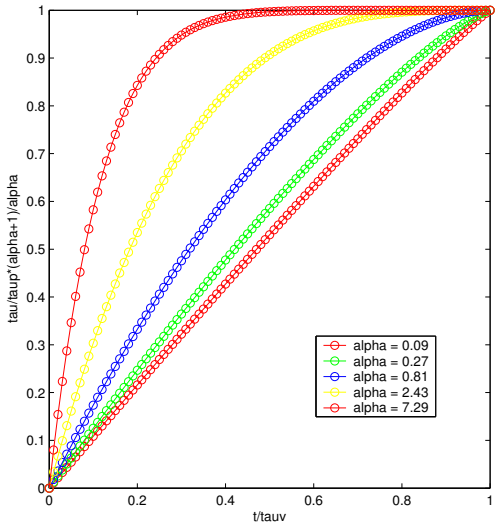


Figure 1: Structure of the change of variable in the evaporating case

4 The non-evaporating case without propagation of the gas velocity

4.1 Numerical investigations

We first investigate the case where there is no propagation speed of the sine gaseous velocity field; the parameter "celer" is then set to zero. We consider a zero initial velocity field, that is $\mathcal{A}^0 = 0$ in (6).

The first conclusion to be drawn from this case is the existence of a limiting value of the product $A\,\tau_p/\lambda$ such that below this value, the characteristic curves do not cross but generate a droplet density exponential increase around the points of zero gaseous velocity and negative gradient. With the taken configuration where $\lambda = 1$ this limiting value is close to 0.04 and we will see that an analytical study yields $1/8\pi$. When then present three cases, the first one is slightly below the limit so that no characteristic crossing can be observed and is presented in Figure 2. When the relaxation time is slightly increased up to 0.5 then one can observed in the caracteristic diagram using the original variables, using the proposed zoom in Figure 3 in the bottom left subplot, the announced crossing, leading to the presence of a shock wave for the semi-kinetic model in the velocity equation and a Dirac "delta shock" in density due to the absence of pressure.

In the configuration of $\tau_p = 1.5$ one can observe the related dynamics in Figure 4 and Figure 5, with $A = 0.1$ and $A = 1.$, which shows that the points where the characteristics cross, the velocity distribution becomes highly non monokinetic, and a pressure term should be introduced in order to control the mass density of droplets (even if at the very point of trajectory crossing the total droplet number density admits a singularity, but not the related kinetic distribution as can be observed in Figure 4 and 5 bottom right subplot, in the phase space for the original variables.

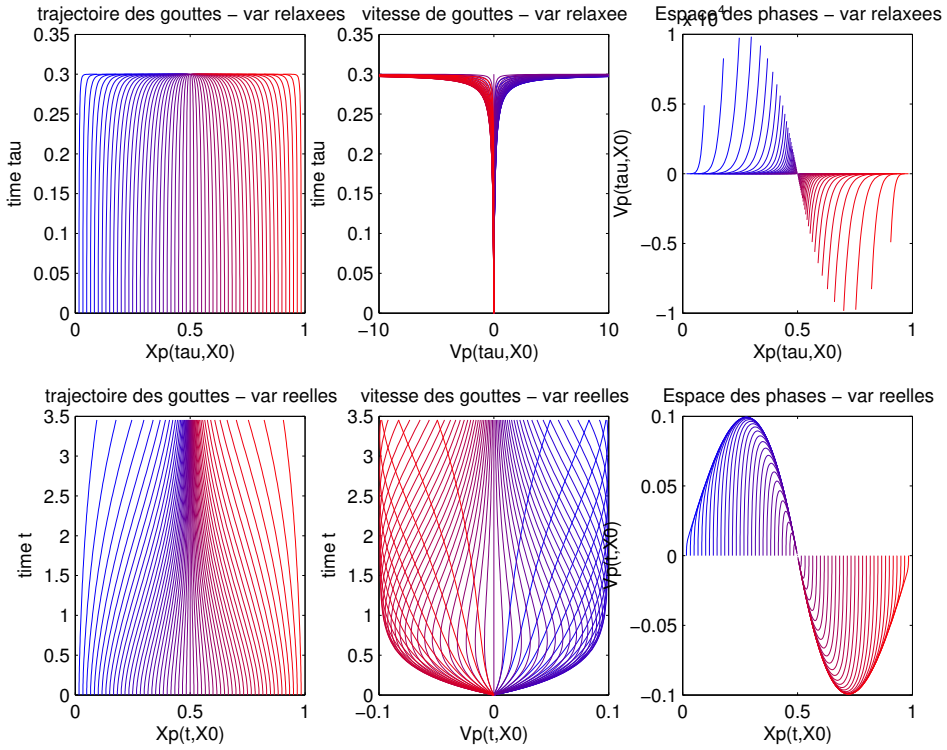


Figure 2: No caracteristic crossing : $\tau_p = 0.3$, $A = 0.1$, and $\lambda = 1$.

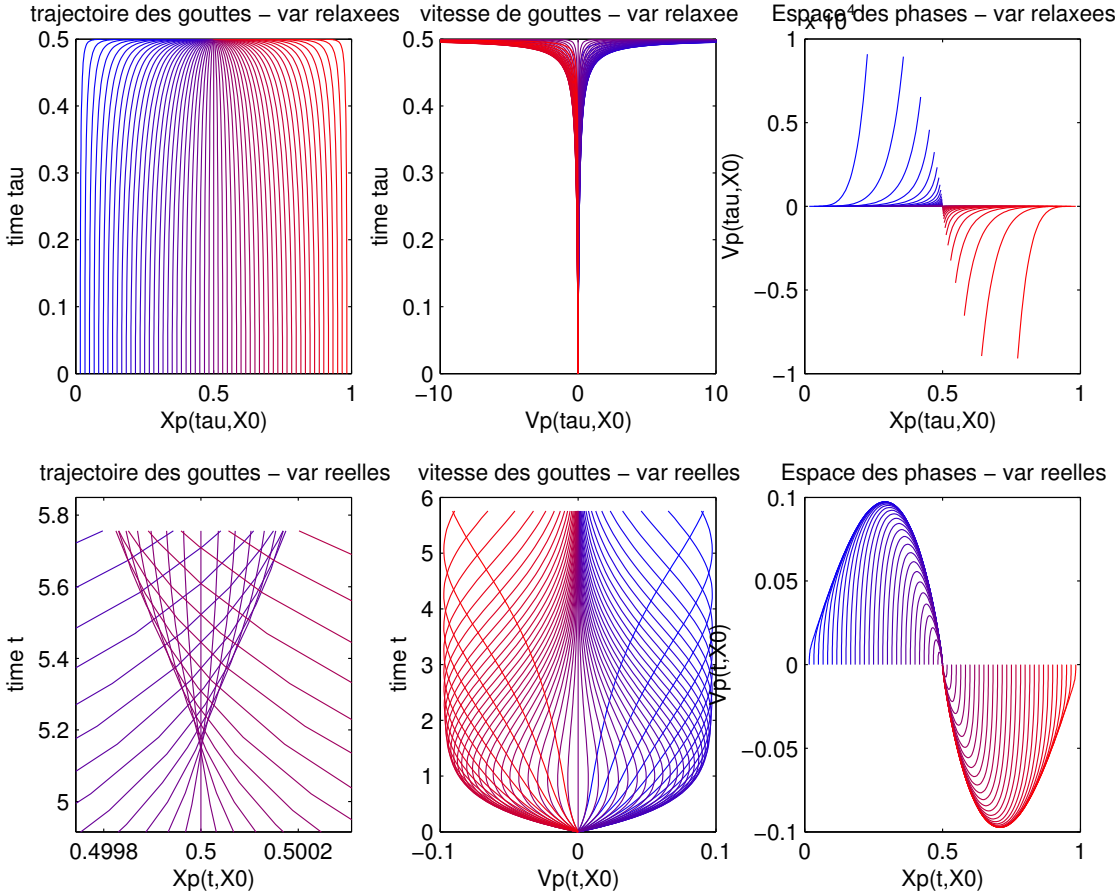


Figure 3: Caracteristic crossing around t=5.2 with $\tau_p = 0.5$, $A = 0.1$, and $\lambda = 1$.

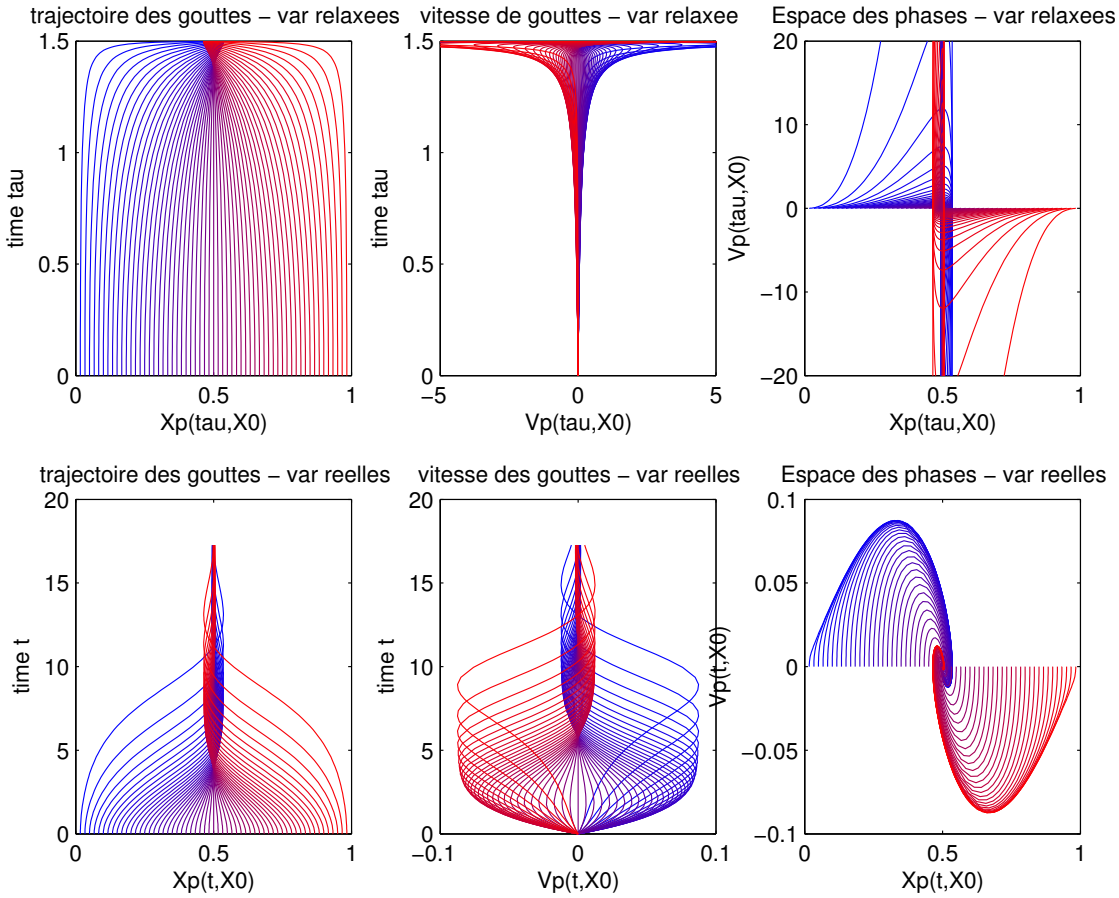


Figure 4: Caracteristic crossing around t=3.83 with $\tau_p = 1.5$, $A = 0.1$, and $\lambda = 1$.

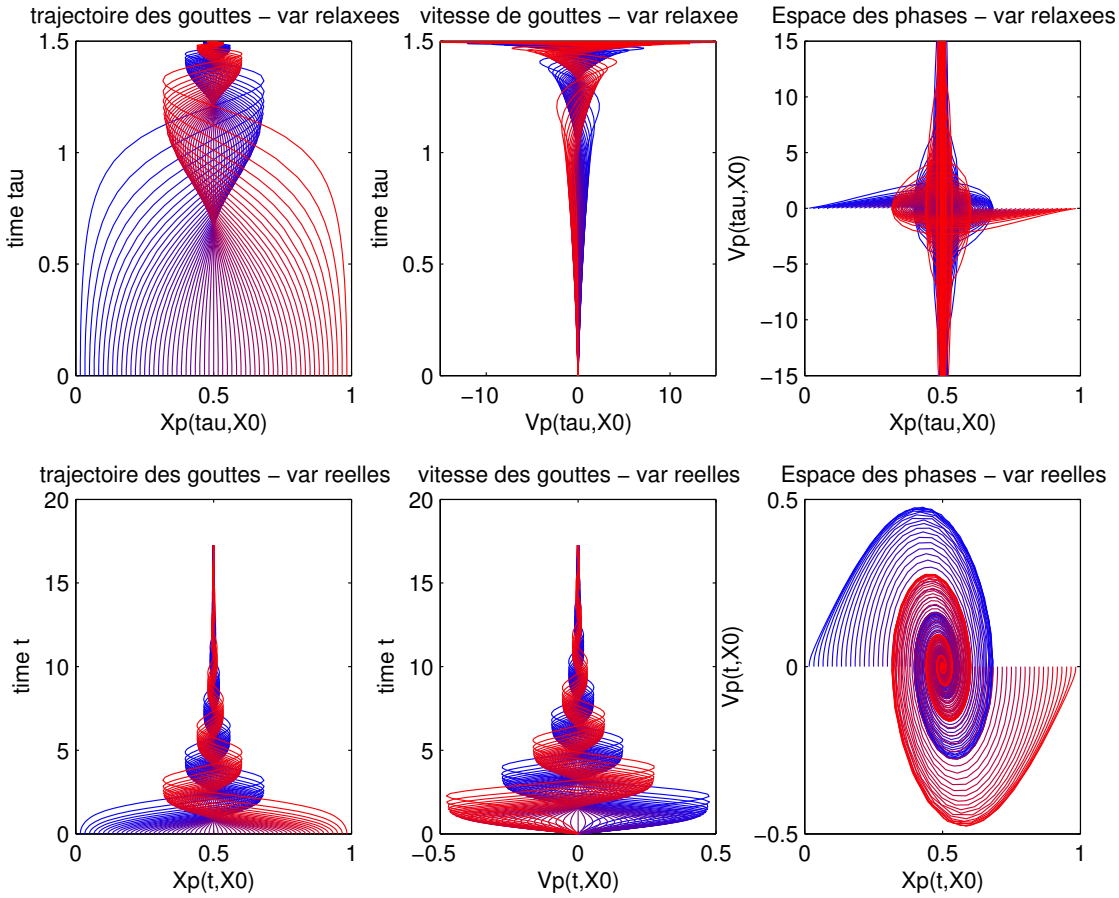


Figure 5: Caracteristic crossing around t=0.87 with $\tau_p = 1.5$, $A = 1.$, and $\lambda = 1$.

4.2 Analysis

Since the caracteristic first crossing point has to be on the center line for which the gaseous velocity is zero as well as the initial droplet velocity, one can try to linearize the original system of ordinary differential equations (7) and to analyze the resulting system of equations. It leads to :

$$\left\{ \begin{array}{ll} \mathrm{d}_t X_p & = V_p, \\ \mathrm{d}_t V_p & = \dfrac{-A\,\frac{2\pi\,X_p}{\lambda} - V_p}{\tau_p(t)}, \end{array} \right. \tag{15}$$

for which the eigenvalues of the associated matrix

$$\begin{bmatrix} 0 & 1 \\ -A\,\dfrac{2\pi}{\lambda\tau_p} & -\dfrac{1}{\tau_p} \end{bmatrix}$$

are real, if and only if

$$8\pi\,A\,\tau_p \leq \lambda. \tag{16}$$

In the case where λ is taken to be 1, the limiting value of $A\,\tau_p$ is then $1/(8\pi) \approx 0.0398$ and we recover the value obtained from the numerical experiments.

4.3 Initial conditions

To take into account the initial velocity conditions is not possible in all its generality. For example, if we take an initial condition with the same amplitude as the one of the gas in a situation where no crossing of the caracteristics is to be expected, then on has a nice pattern appearing in Figure 4.3, but still no crossing of the trajectories; however, if one doubles the amplitude of the initial velocity profile, then some crossing will be generated, but solely by the initial velocity conditions as shown in Figure 4.3.

It is then interesting to notice the only influence of the initial condition when the gaseous velocity is uniformly zero. In this case one notices that the trajectories or characteristics are straight lines in the relaxation variables and the point of shock formation is known analytically and come from the point of minimal derivative in the initial solution

$$\tau_{\text{shock}} = -\frac{1}{\min v_d^{0\prime}} = \frac{\lambda}{2\pi\,r\,\mathrm{A}^0} \tag{17}$$

This yields $\tau \approx 0.265$ and then $t = 0.435$ which fully corresponds to what is observed in Figure 4.3. Besides this particular case admits an analytical solution.

5 The non-evaporating case with propagation of the gas velocity

We consider the influence, for a given τ_p set to the value 1, of the propagation velocity of the sine function associated to the gaseous velocity. Asymptotically, there is an oscillating state for the velocity evolution, the amplitude of which is directly related to the τ_p of the droplets, to the amplitude of the oscillating gaseous velocity A and finally to the propagation velocity c. This amplitude then determines a mean motion of the droplets following the direction of propagation,

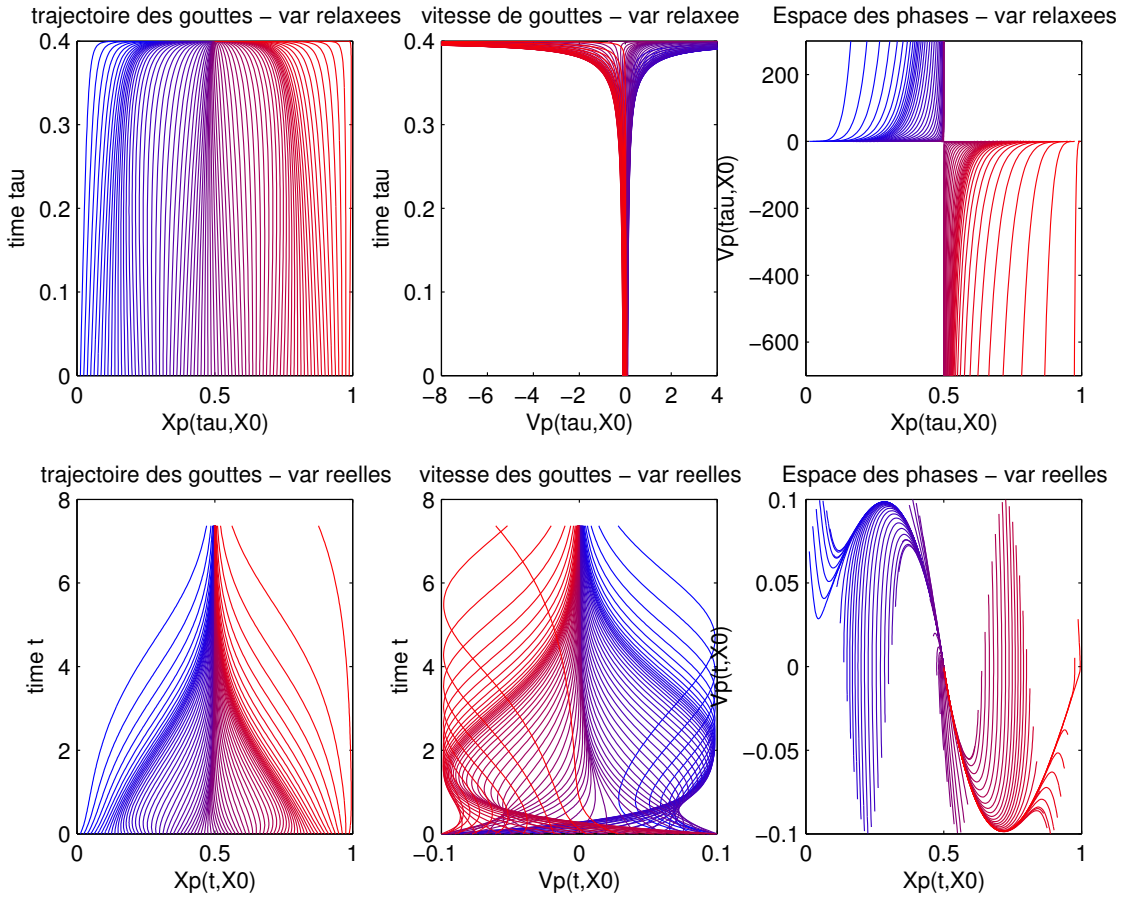


Figure 6: No Caracteristic crossing with $\tau_p = 0.4$, $A = 0.1$, $\lambda = 1$, $\mathcal{A}^0 = 0.1$, $\phi = \pi/6$ and $r = 3$.

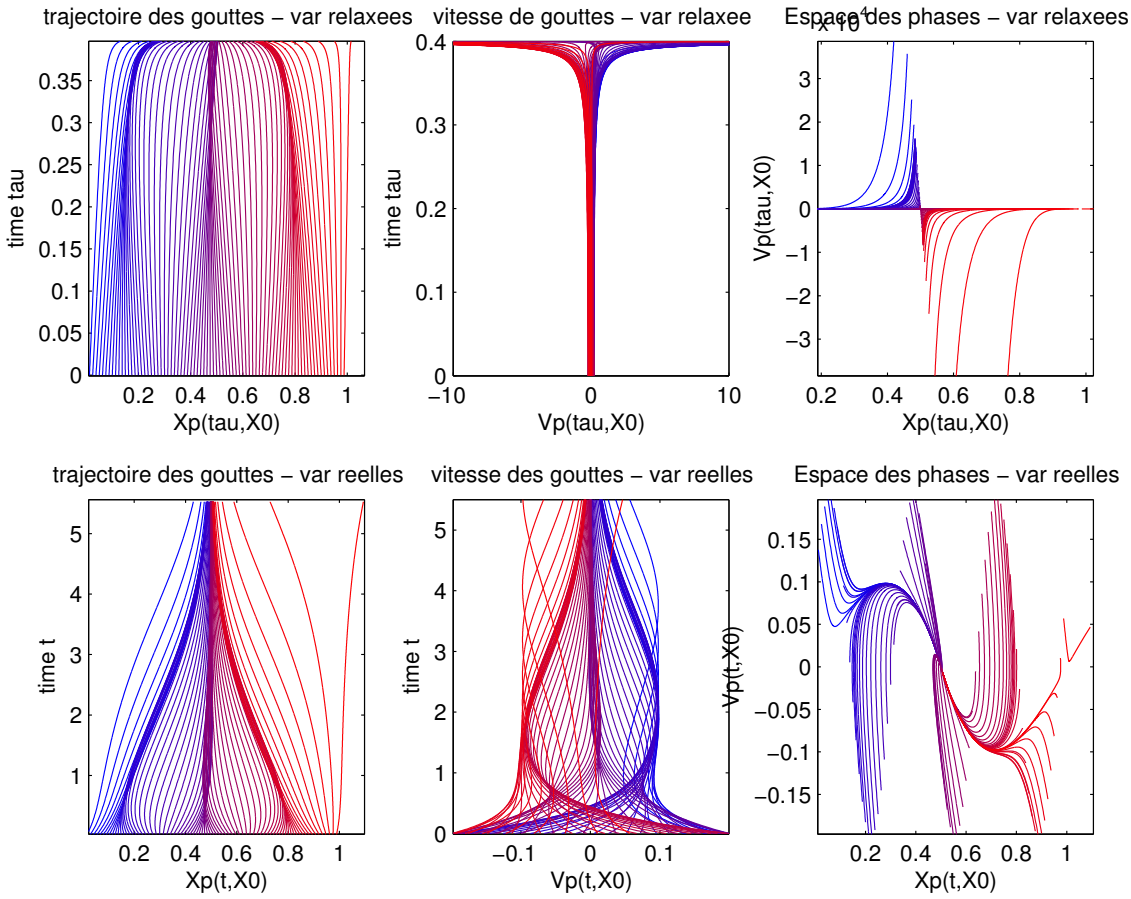


Figure 7: Caracteristic crossing around t=0.4 with $\tau_p = 0.4$, $A = 0.1$, $\lambda = 1$, $\mathcal{A}^0 = 0.2$, $\phi = \pi/6$ and $r = 3$.

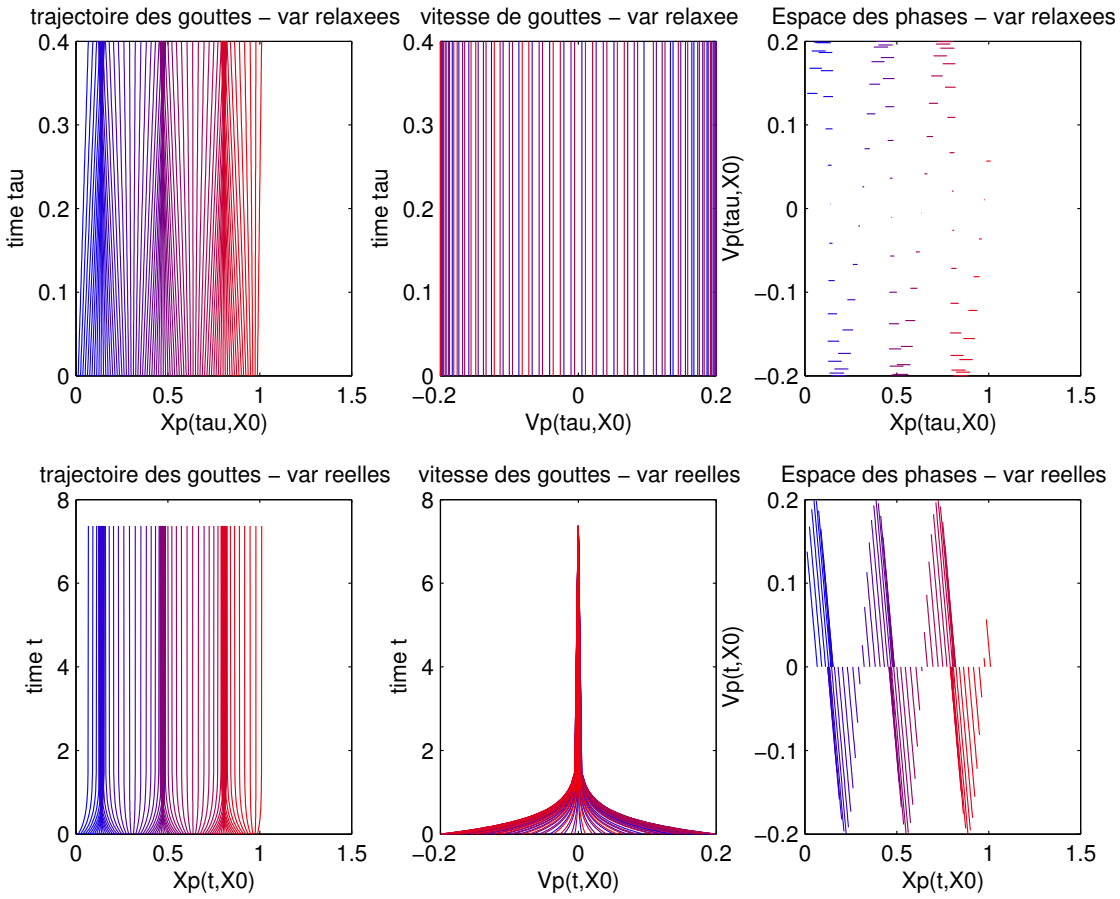


Figure 8: Caracteristic crossing around t=0.4 with $\tau_p = 0.4$, $A = 0$, $\lambda = 1$, $\mathcal{A}^0 = 0.2$, $\phi = \pi/6$ and $r = 3$.

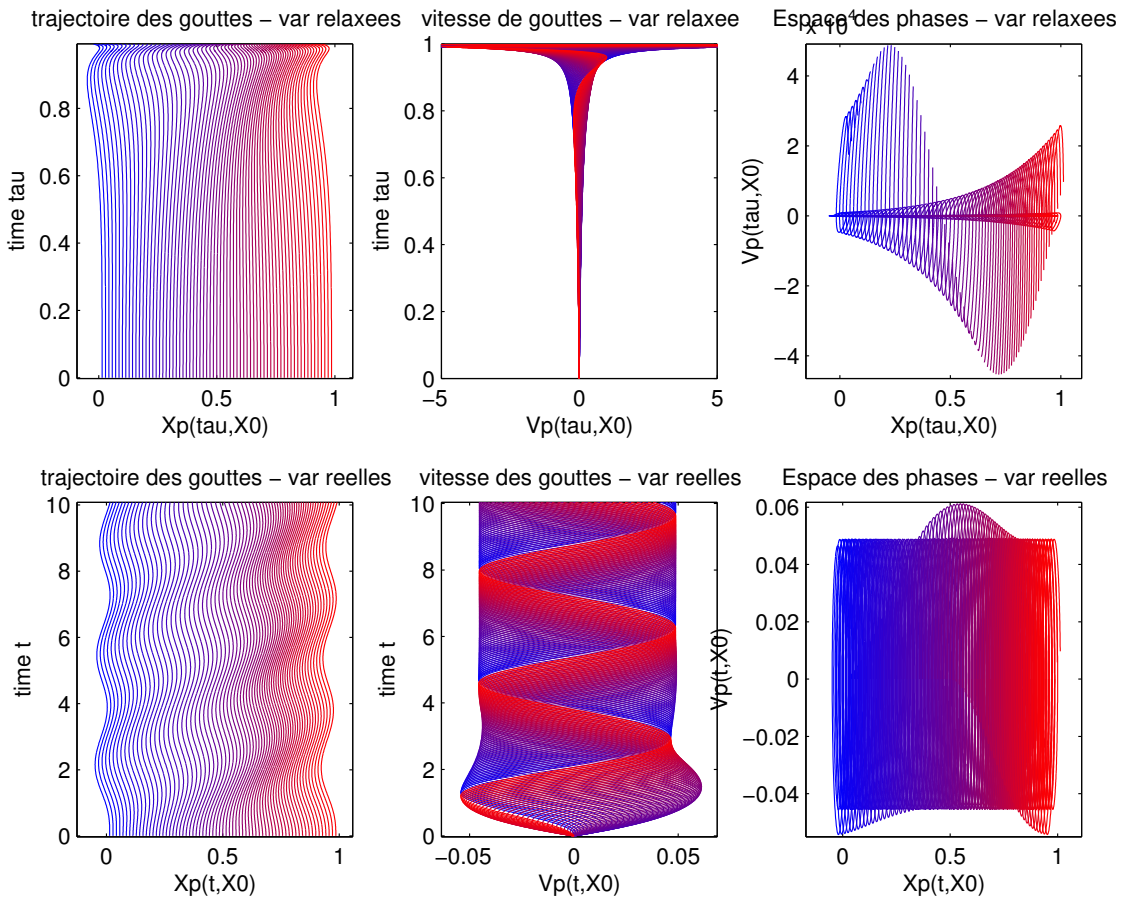


Figure 9: Weak oscillations and propagation in the mean for droplets with $\tau_p = 1.$, $A = 0.1$, $c = 0.3$, $\lambda = 1$ and $\mathcal{A}^0 = 0$.

which is lower for high propagation velocities, as well as the velocity of some dense patterns which propagate at the velocity propagation velocity. The intensity of this "dense patterns" will increase as the maximal droplet velocities in the periodic regime come closer to the propagation velocity as it is shown in Figures 5 - 5. Besides, one can notice a motion of the droplets in the mean which increases as the amplitude of the propagating velocity is increased. It is only the initial velocity distribution that "distributes" the amount of droplets among the patterns presented in the Figure 5 - 5 In Figure 5, the distribution is rather uniform, but as A is increased, we start having some concentration of droplets at some identified location 5, and then some trajectory crossing occurs in Figure 5. However, the droplet velocity never reaches the propagation one, except if the initial conditions in velocity are set in such a way that some droplets are "stuck" in the travelling wave such as in Figure 5 and Figures 5 and 5.

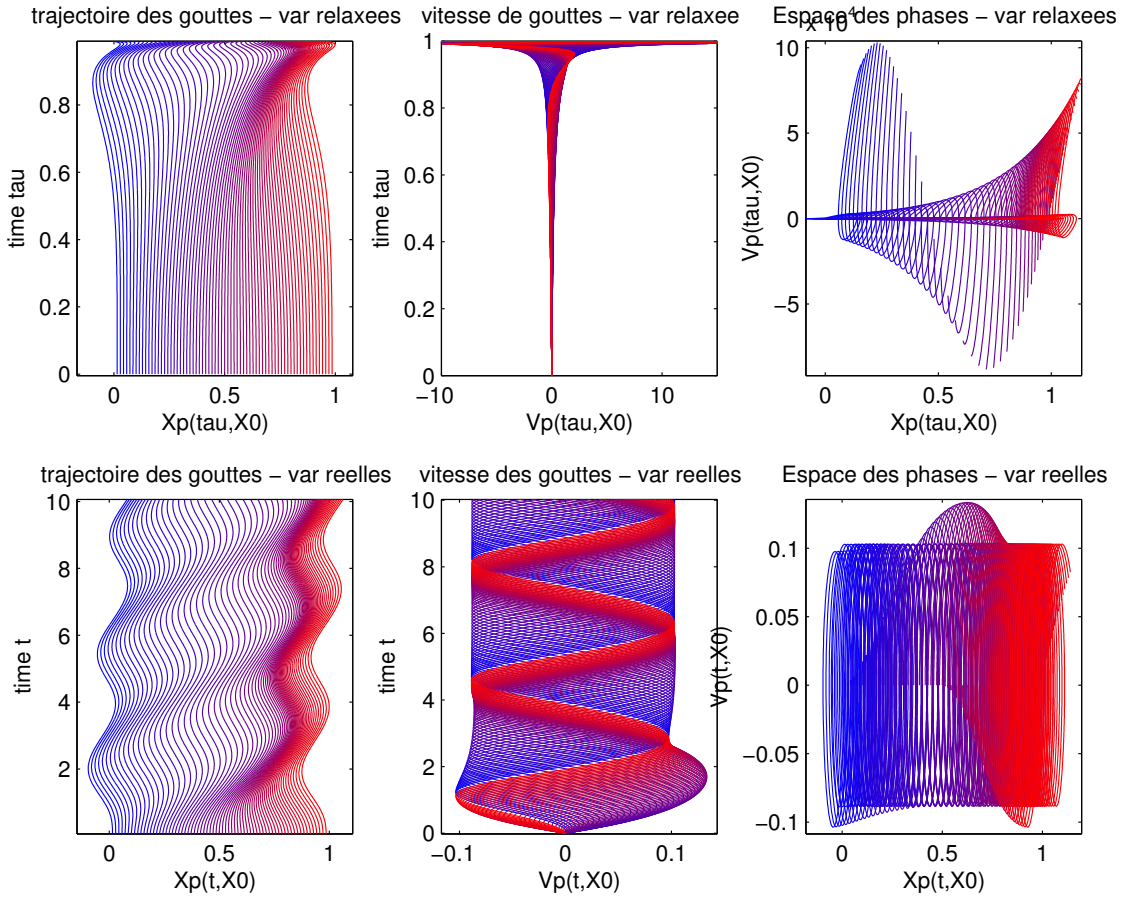


Figure 10: Oscillations and propagation with $\tau_p = 1.$, $A = 0.2$, $c = 0.3$, $\lambda = 1$ and $\mathcal{A}^0 = 0$.

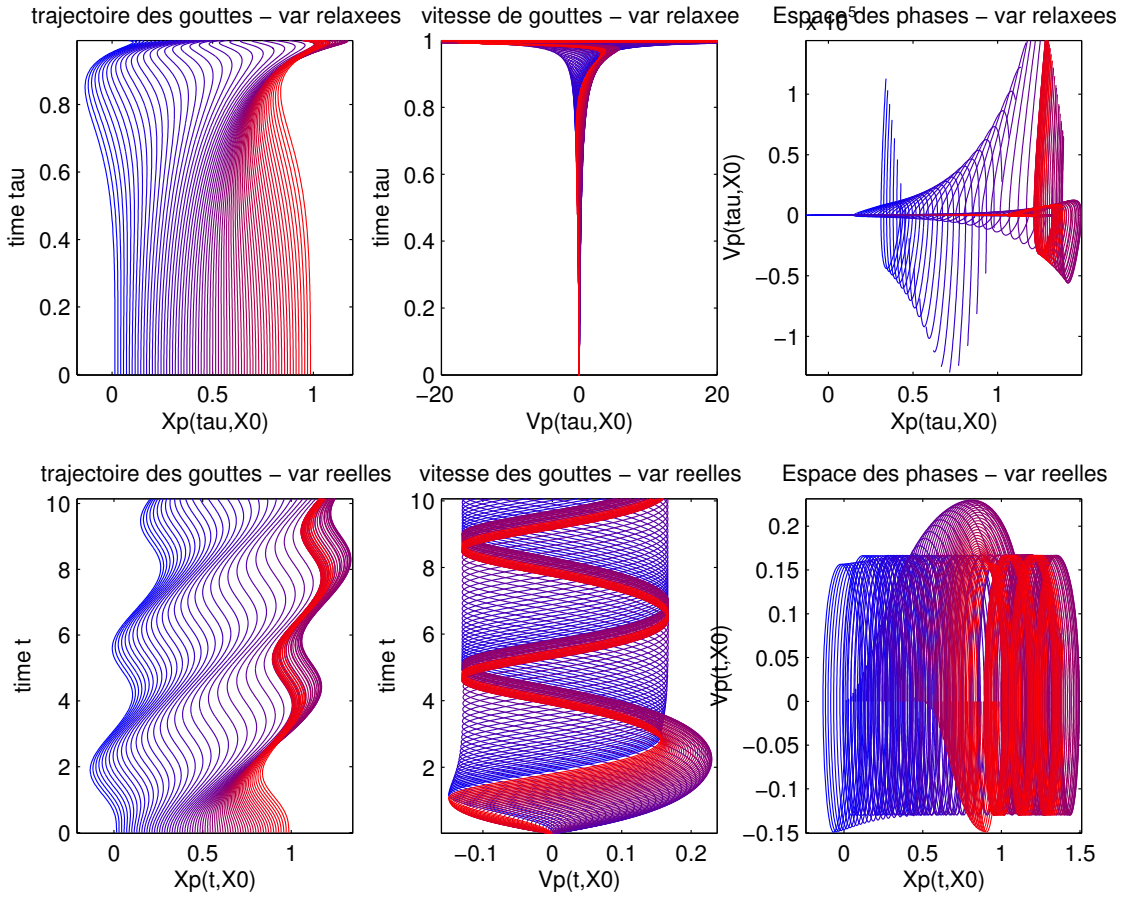


Figure 11: Caracteristic crossing and repartition of droplet number density with $\tau_p = 1.$, $A = 0.3$, $c = 0.3$, $\lambda = 1$ and $\mathcal{A}^0 = 0$.

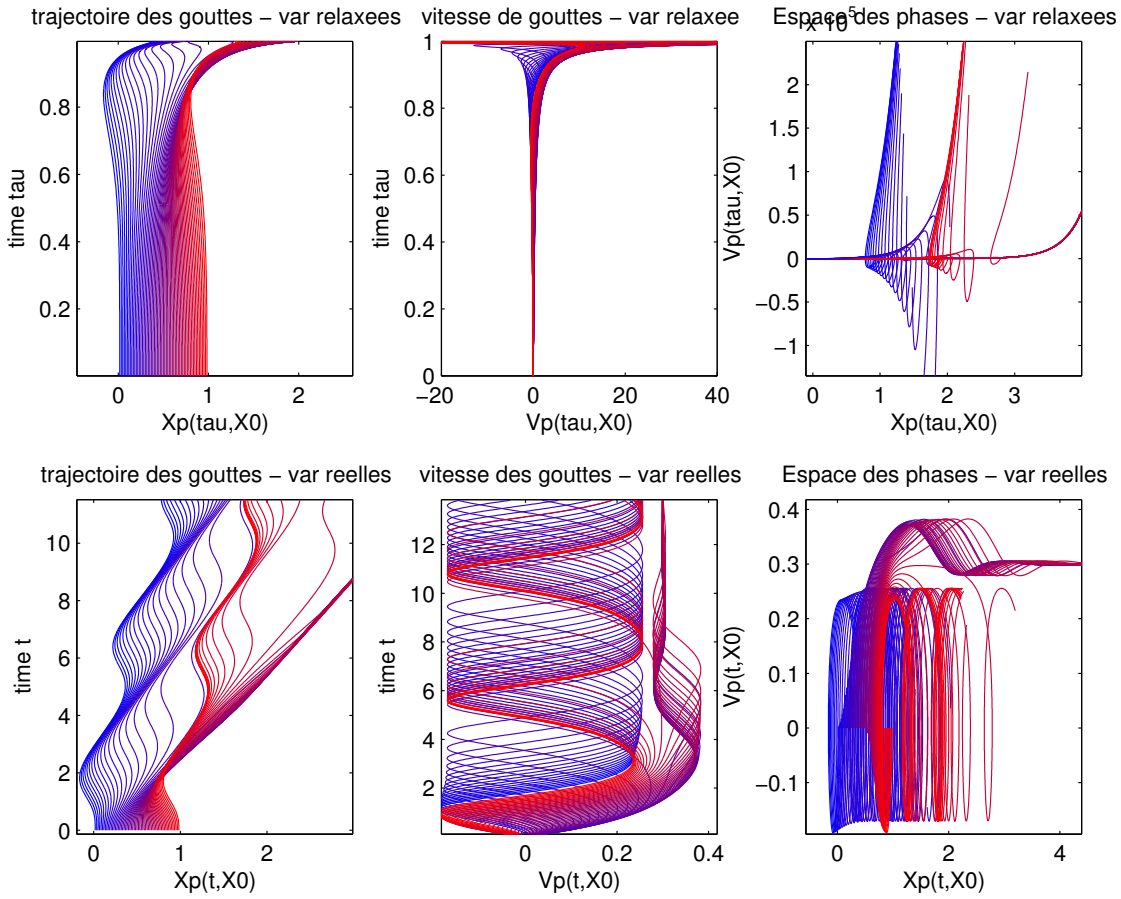


Figure 12: Caracteristic crossing as well as some ejection of droplets with $\tau_p = 1.$, $A = 0.4$, $c = 0.3$, $\lambda = 1$ and $\mathcal{A}^0 = 0$.

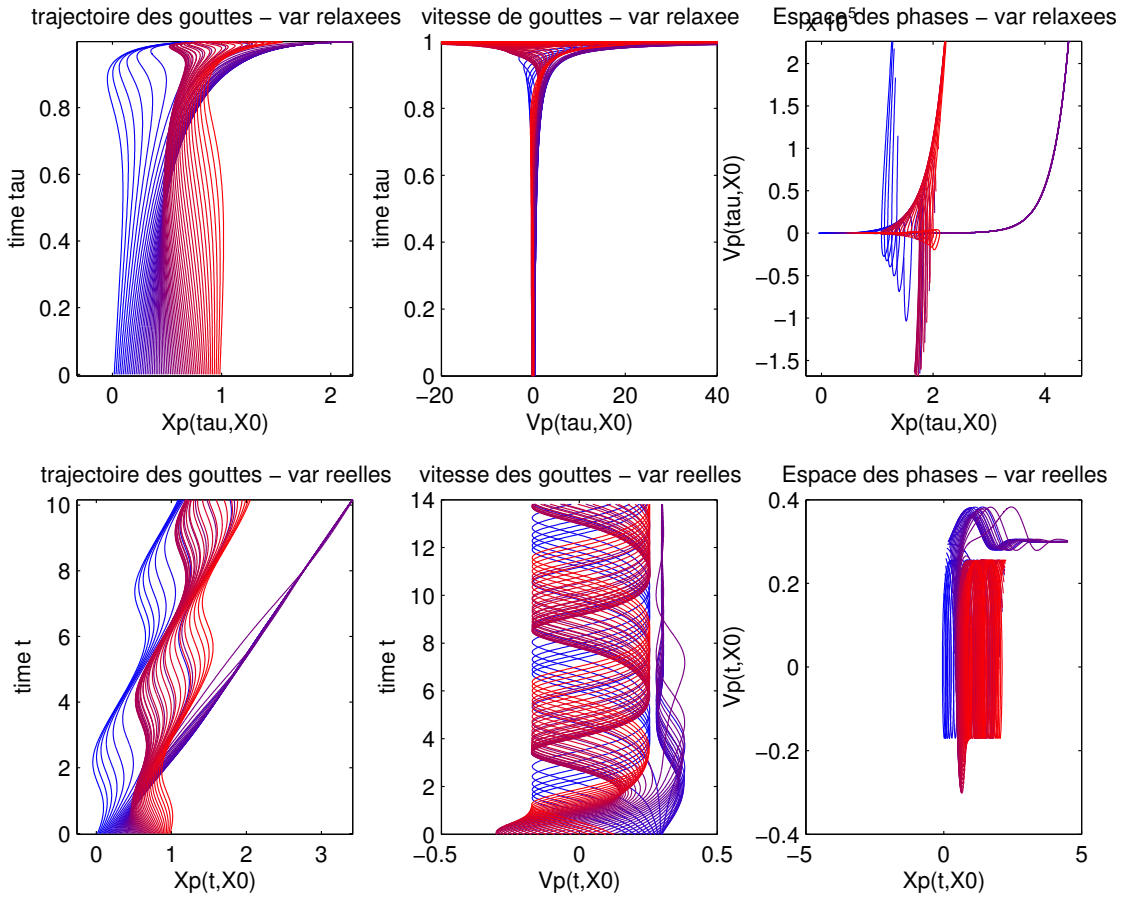


Figure 13: Influence of the initial condition with $\tau_p = 1.$, $A = 0.4$, $c = 0.3$, $\lambda = 1$ and $\mathcal{A}^0 = 0.3$, $\phi = \pi/6$ and $r = 1$

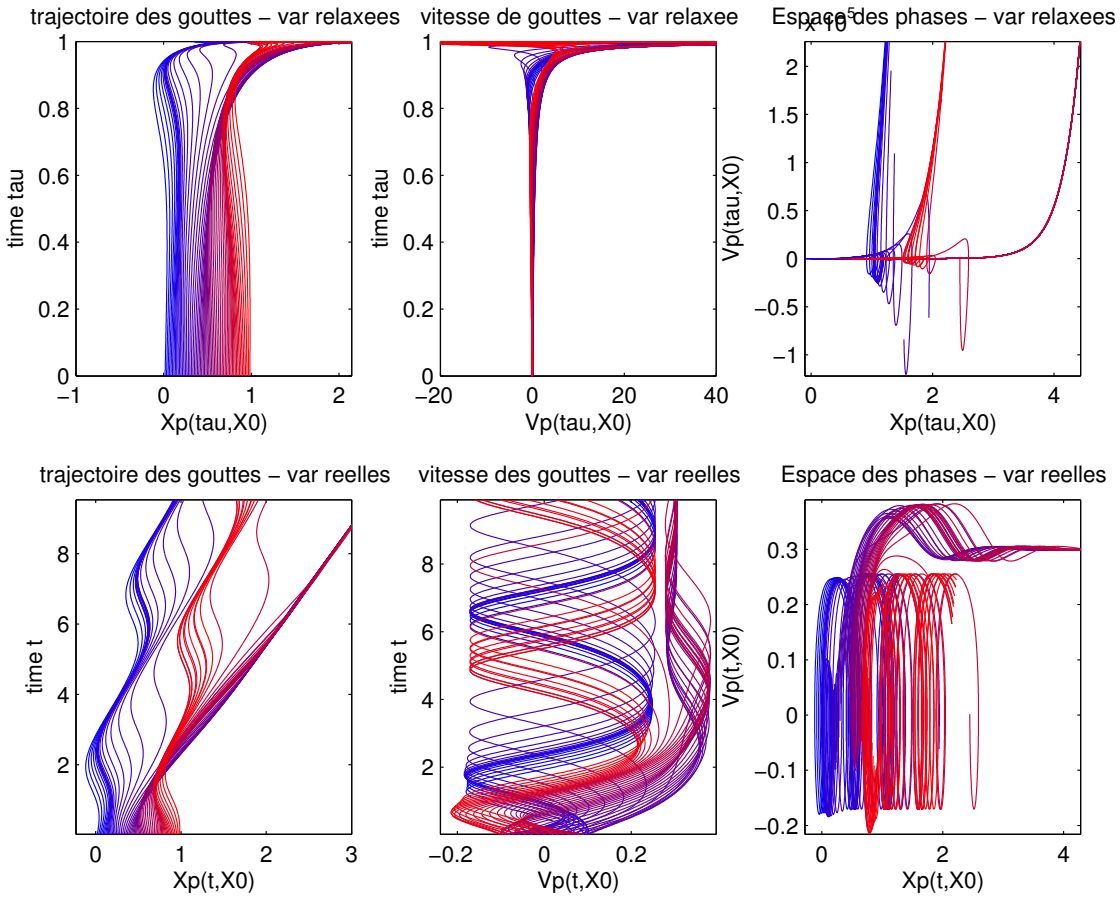


Figure 14: Influence of the initial condition with $\tau_p = 1.$, $A = 0.4$, $c = 0.3$, $\lambda = 1$ and $\mathcal{A}^0 = 0.3$, $\phi = \pi/6$ and $r = 3$